

## Correlated polarons in dissimilar perovskite manganites

C. S. Nelson,<sup>1</sup> M. v. Zimmermann,<sup>1</sup> Y. J. Kim,<sup>1</sup> J. P. Hill,<sup>1</sup> Doon Gibbs,<sup>1</sup> V. Kiryukhin,<sup>2</sup> T. Y. Koo,<sup>2,3</sup> S.-W. Cheong,<sup>2,3</sup> D. Casa,<sup>4</sup> B. Keimer,<sup>5</sup> Y. Tomioka,<sup>6</sup> Y. Tokura,<sup>6,7</sup> T. Gog,<sup>8</sup> and C. T. Venkataraman<sup>8</sup>

<sup>1</sup>*Department of Physics, Brookhaven National Laboratory, Upton, New York 11973-5000*

<sup>2</sup>*Department of Physics and Astronomy, Rutgers University, Piscataway, New Jersey 08854*

<sup>3</sup>*Bell Laboratories, Lucent Technologies, Murray Hill, New Jersey 07974*

<sup>4</sup>*Department of Physics, Princeton University, Princeton, New Jersey 08544*

<sup>5</sup>*Max-Planck-Institut für Festkörperforschung, D-70569, Stuttgart, Germany*

<sup>6</sup>*Joint Research Center for Atom Technology (JRCAT), Tsukuba 305-0033, Japan*

<sup>7</sup>*Department of Applied Physics, University of Tokyo, Tokyo 113-0033, Japan*

<sup>8</sup>*CMC-CAT, Advanced Photon Source, Argonne National Laboratory, Argonne, Illinois 60439*

(Received 30 November 2000; published 2 October 2001)

We report x-ray scattering studies of broad peaks located at  $(0.5\ 0\ 0)/(0\ 0.5\ 0)$ -type wave vectors in the paramagnetic insulating phases of  $\text{La}_{0.7}\text{Ca}_{0.3}\text{MnO}_3$  and  $\text{Pr}_{0.7}\text{Ca}_{0.3}\text{MnO}_3$ . We interpret the scattering in terms of correlated polarons and measure isotropic correlation lengths of 1-2 lattice constants in both samples. Remarkably, the size of these correlated polarons remains constant over the entire temperature range investigated. In  $\text{La}_{0.7}\text{Ca}_{0.3}\text{MnO}_3$ , this range extends up to  $\sim 400$  K, at which temperature the peaks are observed to disappear. Based on the wavevector, the correlated polarons are found to be consistent with a CE-type structure. Differences in behavior between the samples arise as they are cooled through their respective transition temperatures and become ferromagnetic metallic ( $\text{La}_{0.7}\text{Ca}_{0.3}\text{MnO}_3$ ) or charge and orbitally ordered insulating ( $\text{Pr}_{0.7}\text{Ca}_{0.3}\text{MnO}_3$ ). Since the primary difference between the two samples is the trivalent cation size, these results illustrate the robust nature of the correlated polarons to variations in the relative strength of the electron-phonon coupling, in contrast to the sensitivity of the low-temperature ground state to such variations.

DOI: 10.1103/PhysRevB.64.174405

PACS number(s): 75.30.Vn, 71.38.-k, 78.70.Ck

The wide variety of ground state phases exhibited by the perovskite manganites ( $R_{1-x}M_x\text{MnO}_3$  where  $R$  and  $M$  are trivalent rare-earth and divalent alkaline cations, respectively) originates in the interplay of the charge, orbital, lattice, and spin degrees of freedom. A related manifestation of this interplay is the colossal magnetoresistance (CMR) effect,<sup>1</sup> a phenomenon that has caused a resurgence of interest in the perovskite manganites due to its potential for technological applications. Recent work has focused on the role of the electron-phonon interaction, which has been used to supplement the double exchange interaction,<sup>2</sup> and is believed to be a necessary ingredient for modeling the temperature dependence of the magnetic and transport behavior of CMR materials.<sup>3,4</sup>

In CMR materials, strong electron-phonon coupling results in the formation of localized charge carriers with associated lattice distortions—or polarons—in the paramagnetic insulating phase. Early evidence of polarons was obtained from transport measurements,<sup>5,6</sup> from which a high-temperature–small-polaron and low-temperature–large-polaron phenomenology was hypothesized. Studies using local probes<sup>7,8</sup> supported this view of the high-temperature, polaronic behavior, and more recently, interest has turned to consideration of polaron-polaron interactions in this temperature regime. One theoretical model, proposed by Alexandrov and Bratkovsky,<sup>9</sup> involves paired polarons, or bipolarons. In this model, strong electron-phonon coupling at high temperatures binds polarons into immobile pairs in a singlet state, with two holes localized on a single oxygen ion. Then, as the temperature is reduced toward  $T_c$ , the ferromagnetic exchange coupling increases in strength and

the bipolarons are broken apart, leaving single polarons in the ferromagnetic metallic phase. Evidence consistent with bipolarons—based on transport measurements of polycrystalline  $\text{La}_{5/8}\text{Ca}_{3/8}\text{MnO}_3$  (Ref. 10) and films of  $\text{La}_{0.75}\text{Ca}_{0.25}\text{MnO}_3$  and  $\text{Nd}_{0.7}\text{Sr}_{0.3}\text{MnO}_3$  (Ref. 11)—has recently been reported, but additional data using more direct techniques are clearly desirable.

X-ray and neutron scattering experiments can make an important contribution to studies of polarons since they are directly sensitive to both the polarons and their correlations. Recently, these techniques were applied to the perovskite manganite  $(\text{Nd}_{0.125}\text{Sm}_{0.875})_{0.52}\text{Sr}_{0.48}\text{MnO}_3$  (Ref. 12) and the layered manganite  $\text{La}_{1.2}\text{Sr}_{1.8}\text{Mn}_2\text{O}_7$ .<sup>13</sup> In both materials, diffuse scattering around the Bragg peaks and well-resolved peaks at incommensurate wavevectors were observed in the high-temperature phases, and both types of scattering were found to disappear as the samples were cooled through  $T_c$ . The two scattering components were attributed to the presence of polarons—the diffuse scattering from single polarons and the resolved peaks from polaron correlations—implying that both polarons and polaron correlations were absent in the ferromagnetic metallic phases. Very recently, neutron scattering studies of the  $\text{La}_{1-x}\text{Ca}_x\text{MnO}_3$  system<sup>14,15</sup> have reported similar results. However, in this case as well as in electron microdiffraction experiments,<sup>16</sup> the correlations were observed at a commensurate wave vector of  $(0.5\ 0\ 0)$  and  $(0\ 0.5\ 0)$ , in orthorhombic notation.

As discussed above, the important parameter controlling the polaron behavior in CMR materials is the electron-phonon coupling. What is missing in the work reported to date is a systematic study of the polarons as a function of the

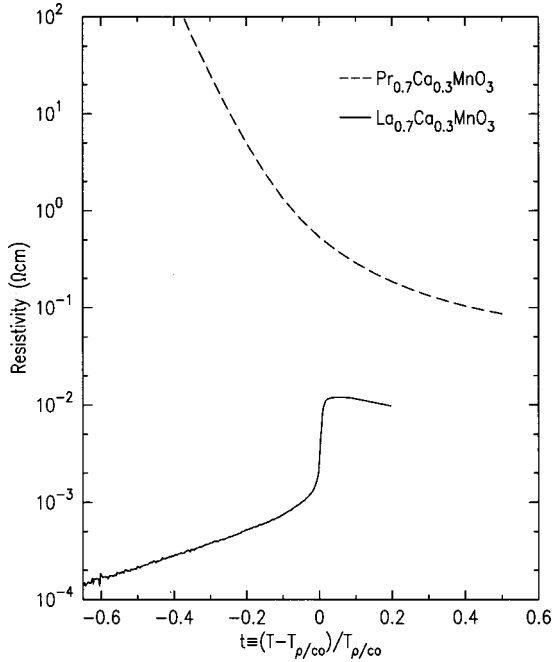


FIG. 1. Resistivity as a function of reduced temperature  $t \equiv (T - T_{\rho/co})/T_{\rho/co}$  in  $\text{La}_{0.7}\text{Ca}_{0.3}\text{MnO}_3$  (solid) and  $\text{Pr}_{0.7}\text{Ca}_{0.3}\text{MnO}_3$  (dashed). Note that the  $\text{Pr}_{0.7}\text{Ca}_{0.3}\text{MnO}_3$  data were obtained using a two-point probe measurement of the resistance, and include an estimated scale factor for the conversion to resistivity.

relative strength of this coupling. In this paper, we take a step in this direction by reporting x-ray scattering studies of two identically doped perovskite manganites, which have different trivalent cations. To first order, such substitution does not affect the charge, orbital, or spin degrees of freedom but only alters the lattice degree of freedom, due to the difference in trivalent cation size. One result of this is a change in the relative strength of the electron-phonon coupling. The systems chosen for this study are  $\text{La}_{1-x}\text{Ca}_x\text{MnO}_3$  and  $\text{Pr}_{1-x}\text{Ca}_x\text{MnO}_3$ , each with a doping of  $x=0.3$ .

$\text{La}_{0.7}\text{Ca}_{0.3}\text{MnO}_3$  and  $\text{Pr}_{0.7}\text{Ca}_{0.3}\text{MnO}_3$  are both paramagnetic insulators at room temperature. Upon cooling, these two materials go through transitions into completely different low-temperature phases—a ferromagnetic metallic phase<sup>17</sup> and an antiferromagnetic, charge and orbitally ordered, insulating phase,<sup>18,19</sup> respectively. The contrasting transport behavior is illustrated by the resistivity measurements displayed in Fig. 1. The origin of the difference in the low-temperature phases is believed to be the  $\sim 3\%$  decrease in cation radius from La to Pr. The smaller Pr ions produce a larger distortion of the Mn-O-Mn bond angles away from  $180^\circ$  [ $156.4^\circ$  for Pr versus  $\sim 160.7^\circ$  for La (Ref. 20)] resulting in a smaller bandwidth and elastic modulus. Both of these effects increase the relative strength of the electron-phonon coupling.<sup>21,3,22</sup>

Here, we report x-ray scattering studies of the polarons in the paramagnetic insulating phases of these dissimilar perovskite manganites. We find that the high-temperature behaviors are insensitive to the variation in the relative strength of the electron-phonon coupling between the two samples. Specifically, in both samples, we observe broad, commensurate

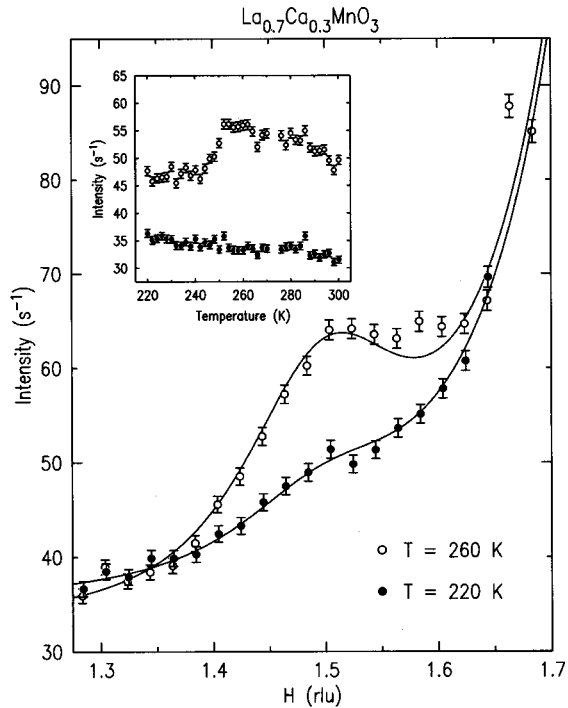
peaks with similar correlation lengths of 1–2 lattice constants. The correlation lengths are observed to be constant over the entire temperature range investigated, which extends up to  $\sim 400$  K—the temperature at which the peaks are observed to disappear—in  $\text{La}_{0.7}\text{Ca}_{0.3}\text{MnO}_3$ . We interpret the peaks in terms of correlated polarons, and based on the wavevector and correlation length, find their structure to be consistent with that of a CE-type orbital order domain. The difference in the relative strength of the electron-phonon coupling in the two samples is only manifested upon cooling through the respective transition temperatures. In  $\text{La}_{0.7}\text{Ca}_{0.3}\text{MnO}_3$ , the broad peak decreases in intensity as the sample becomes ferromagnetic metallic, while in  $\text{Pr}_{0.7}\text{Ca}_{0.3}\text{MnO}_3$ , the peak narrows and increases in intensity as the sample enters a CE-type orbitally ordered domain state.

The  $\text{La}_{0.7}\text{Ca}_{0.3}\text{MnO}_3$  and  $\text{Pr}_{0.7}\text{Ca}_{0.3}\text{MnO}_3$  single crystals used in this study were grown by floating zone techniques at Bell Laboratories and JRCAT, respectively. The x-ray scattering measurements were carried out on beamline X22C at the National Synchrotron Light Source (NSLS) and beamline 9ID at the Advanced Photon Source. The low-temperature work was performed using a closed-cycle refrigerator. For the high-temperature measurements of  $\text{La}_{0.7}\text{Ca}_{0.3}\text{MnO}_3$ , the sample was placed in a furnace in an air atmosphere in order to prevent the possible loss of oxygen. Both samples were determined to be fully twinned, with (110)/(002)-oriented surface normals (in orthorhombic,  $Pbnm$  notation) and mosaic widths of  $\sim 0.2^\circ$  (FWHM). For simplicity, all reflections discussed here are referenced using the (110) surface normal direction.

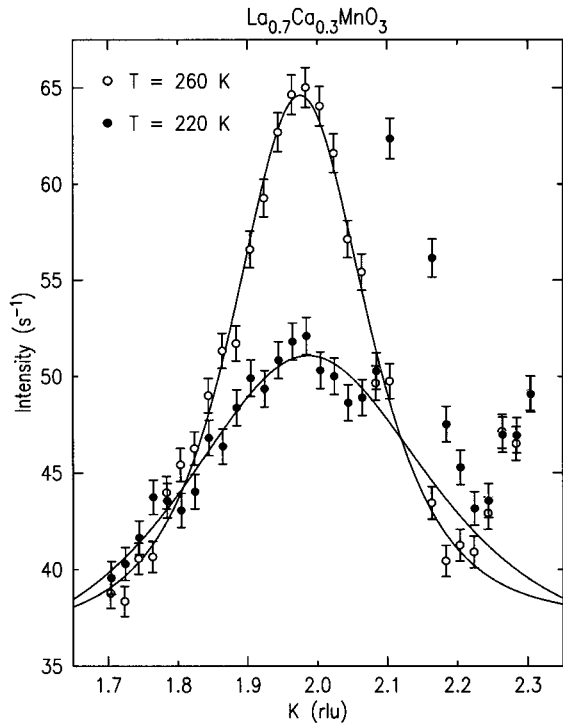
We begin with the  $\text{La}_{0.7}\text{Ca}_{0.3}\text{MnO}_3$  sample. Just above the metal-insulator transition temperature of  $\sim 252$  K ( $T_\rho$ ), broad peaks with ordering wave vectors of (0.5 0 0) and (0 0.5 0) and peak intensities of  $\sim 20$  counts/s were observed (with an incident photon energy of 6.535 keV on beamline X22C at the NSLS). Note that twinning of the sample and the width of the peaks make it impossible to determine whether or not there is a unique ordering wavevector. As the sample was cooled through the transition temperature into the ferromagnetic metallic phase, the peaks abruptly decreased in intensity [see inset to Fig. 2(a)]. Two temperature snapshots of this behavior at 260 and 220 K are shown in Fig. 2.

Reciprocal space mesh scans around the (220) and (440) Bragg peaks were carried out at 260 and 220 K. Diffuse scattering consistent with the neutron scattering work reported by Dai *et al.*<sup>14</sup> and Adams *et al.*<sup>15</sup> was observed around the (440) Bragg peak, with a similar change in intensity and shape. We attribute the apparent absence of temperature-dependent diffuse scattering around the (220) Bragg peak to the  $(\mathbf{Q} \cdot \boldsymbol{\delta})^2$  variation in the scattering intensity from a lattice distortion, in the limit of small displacement  $\boldsymbol{\delta}$ .

The temperature dependence of the broad peak was studied using reciprocal space scans along  $H$  and  $K$ , between temperatures of 220 and 400 K. Data from 220 to 300 K were collected at (1.5 2 0), and above room temperature, at (4 4.5 0). Fitting the data to a Lorentzian-squared line shape provides information about the correlation lengths along the orthorhombic  $a$  and  $b$  directions. The correlation lengths are



(a)



(b)

FIG. 2.  $H$  (a) and  $K$  (b) reciprocal space scans through  $(1.5\ 2\ 0)$  in  $\text{La}_{0.7}\text{Ca}_{0.3}\text{MnO}_3$ . Data were measured at temperatures of 260 K (open) and 220 K (closed), and were fit with a Lorentzian-squared line shape (line). The peaks at  $(1.67\ 2\ 0)$  and  $(1.5\ 2.13\ 0)$  arise from powder lines that are believed to be associated with the copper sample holder, and were excluded from the fits. Inset of (a) shows temperature dependence of scattering intensity at  $(1.5\ 2\ 0)$  (open) and  $(1.3\ 2\ 0)$  (closed).

defined as  $\xi_a \equiv a/2\pi\Delta H$  and  $\xi_b \equiv b/2\pi\Delta K$ , where  $a$  and  $b$  are the lattice constants and  $\Delta H$  and  $\Delta K$  are the half-width-at-half-maximum (HWHM) values of the diffuse peaks along  $H$  and  $K$ , respectively. Between  $T_p = 252$  and 400 K, the correlation lengths of the diffuse peak were observed to be independent of temperature, with a magnitude of 1–2 lattice constants. The peak intensity was observed to decrease with increasing temperature, and to reach the limits of detectability at  $\sim 400$  K. Transverse scans, performed between 220 and 300 K, demonstrated that the correlations are isotropic.

Turning now to  $\text{Pr}_{0.7}\text{Ca}_{0.3}\text{MnO}_3$ , the  $x=0.3$  doping in this system lies near the phase boundary between the CE-type charge and orbitally ordered, antiferromagnetic, insulating phase ( $T_{co} \approx 220$  K,  $T_N \approx 150$  K) and a ferromagnetic insulating phase ( $T_c \approx 140$  K).<sup>19</sup> Because of the close proximity to different low-temperature phases—coupled with recent reports of phase separation at this doping<sup>23,24</sup>—we first carried out measurements at low temperatures ( $\sim 100$  K) with a high-resolution Ge(111) analyzer in order to characterize the low-temperature behavior. Three ordered phases associated with at least two different crystallographic phases were observed. Two of these ordered phases are consistent with a CE-type charge and orbital order structure—with  $(100)/(010)$  and  $(0.5\ 0\ 0)/(0\ 0.5\ 0)$  wave vectors, respectively—while the third exhibited only a  $(100)/(010)$  ordering wave vector. The distinct nature of the three phases was determined via measurements of their respective temperature dependences. The two CE-type phases were found to have ordering transitions at 130 and 200 K, respectively, while ordering in the third phase persisted up to 300 K. For the purposes of this paper, we focus on the CE-type phase with the higher transition temperature in what follows, since its behavior is consistent

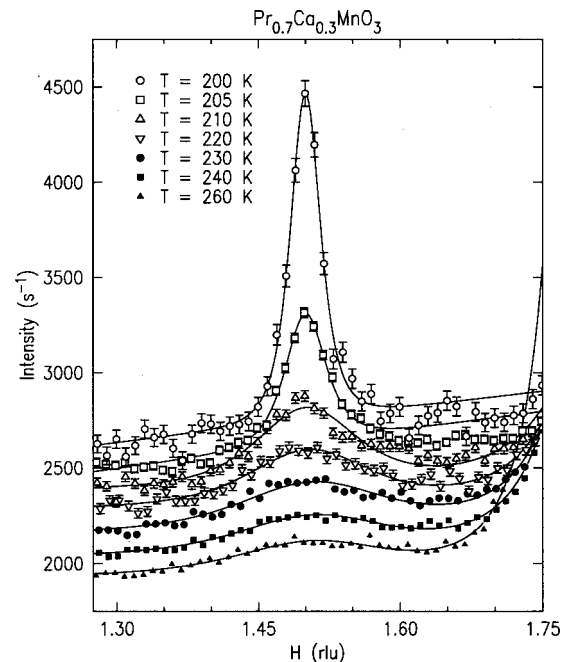


FIG. 3. Temperature dependence of the scattering at  $(H\ 2\ 0)$ , shown with Lorentzian-squared fits (solid), in  $\text{Pr}_{0.7}\text{Ca}_{0.3}\text{MnO}_3$ . For clarity, each data set and fit is shifted upward by  $125\ \text{s}^{-1}$  with respect to the next higher temperature data set and fit.

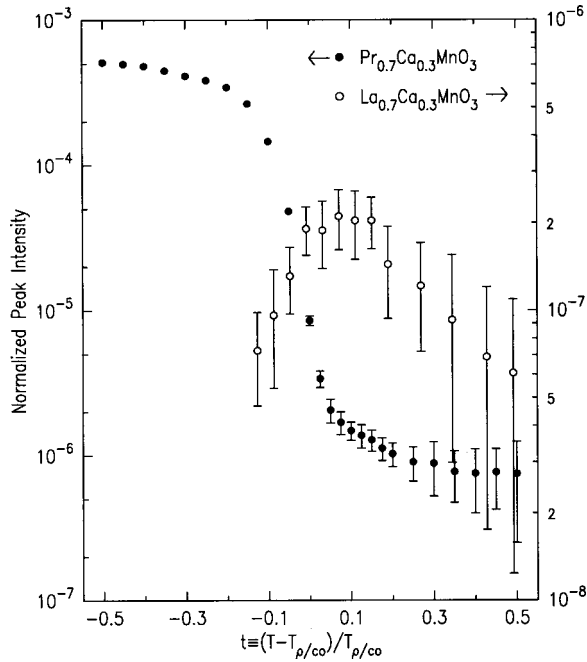


FIG. 4. Peak intensity of the (0.5 0 0)/(0.5 0)-type scattering—normalized to the (2 2 0) Bragg peak intensity at 220 K ( $\text{La}_{0.7}\text{Ca}_{0.3}\text{MnO}_3$ ) and 100 K ( $\text{Pr}_{0.7}\text{Ca}_{0.3}\text{MnO}_3$ )—as a function of reduced temperature  $t \equiv (T - T_{\rho/co})/T_{\rho/co}$ , in  $\text{La}_{0.7}\text{Ca}_{0.3}\text{MnO}_3$  (open) and  $\text{Pr}_{0.7}\text{Ca}_{0.3}\text{MnO}_3$  (closed). The data for  $T \geq 300$  K of  $\text{La}_{0.7}\text{Ca}_{0.3}\text{MnO}_3$  were scaled to match the low-temperature data at 300 K.

with previous studies of  $\text{Pr}_{0.7}\text{Ca}_{0.3}\text{MnO}_3$ .<sup>19</sup> A complete analysis of the phase separation in  $\text{Pr}_{0.7}\text{Ca}_{0.3}\text{MnO}_3$  will be presented in a future paper.<sup>25</sup>

The (1.5 2 0) orbital order peak was measured while warming the sample up to the ordering temperature of  $\sim 200$  K. At low temperatures, the peak width was measured using a Ge(111) analyzer, and a correlation length of  $170 \pm 20$  Å was determined. As the sample temperature was increased through the ordering temperature, the (1.5 2 0) intensity decreased dramatically, as shown in Fig. 3. The peak was also observed to broaden rapidly, reaching a value corresponding to a correlation length of 1–2 lattice constants at high temperatures.

To quantitatively compare the two samples, both data sets were analyzed by fitting to a double Lorentzian-squared line shape.<sup>26</sup> This procedure enabled the diffuse (0.5 0 0)/(0.5 0)-type peaks to be separated out from the tails of the nearby Bragg peak. The results of these fits are summarized in Figs. 4 and 5, showing the normalized peak intensity and the HWHM, respectively, versus reduced temperature. In each case, the reduced temperature  $t$  is defined as  $(T - T_{\rho/co})/T_{\rho/co}$ , where  $T_{\rho/co}$  is the metal-insulator ( $\text{La}_{0.7}\text{Ca}_{0.3}\text{MnO}_3$ ) or charge and orbital order ( $\text{Pr}_{0.7}\text{Ca}_{0.3}\text{MnO}_3$ ) transition temperature.

With regard to both intensities and correlation lengths, the scattering due to correlated polarons in the two samples exhibits strikingly similar behavior above the respective transition temperatures. That is, the intensities decrease gradually with increasing temperature, and the correlation lengths re-

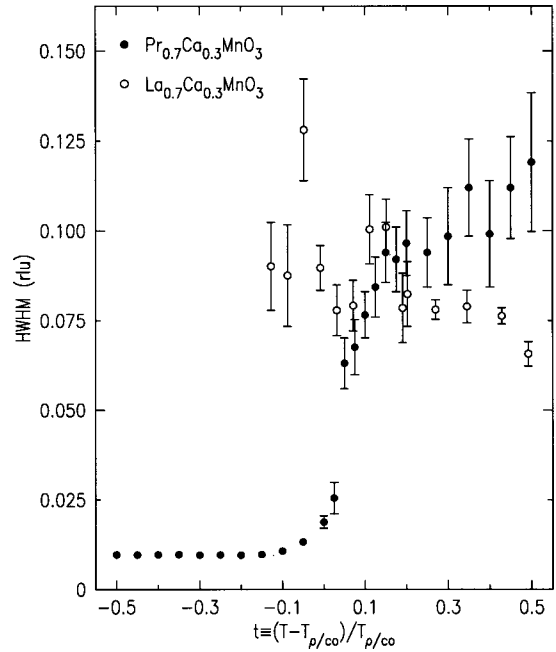


FIG. 5. The fitted half-widths of the (0.5 0 0)/(0.5 0)-type scattering as a function of reduced temperature  $t \equiv (T - T_{\rho/co})/T_{\rho/co}$ , in  $\text{La}_{0.7}\text{Ca}_{0.3}\text{MnO}_3$  (open) and  $\text{Pr}_{0.7}\text{Ca}_{0.3}\text{MnO}_3$  (closed).

main on the order of 1–2 lattice constants up to the highest temperatures studied. The dependence of the scattered intensity on incident photon energy at the (1.5 2 0) peak was also found to be similar in the two samples. Specifically, the intensity exhibited a sharp drop near the Mn K edge, consistent with normal charge scattering, and indicating that the scattering at this  $Q$  is primarily due to lattice distortions in both samples.

In the paramagnetic insulating phases of both samples, the magnitude of the wave vector and the size and stability of the correlation lengths suggest an additional conclusion—that the correlations arise from the presence of composite objects. We label these objects “CE-type bipolarons,” based on the proposed structure that is displayed in Fig. 6. The structure is

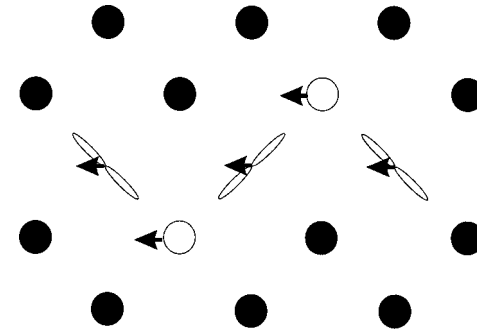


FIG. 6. Schematic diagram of the structure of a CE-type bipolaron, in the  $a$ - $b$  plane. Open circles represent  $\text{Mn}^{4+}$  ions; elongated figure-eights represent the occupied  $e_g$  ( $3d_{z^2-r^2}$ ) orbital of  $\text{Mn}^{3+}$  ions; closed circles represent Mn ions that, on average, have the formal valence and no net orbital order; and arrows indicate the in-plane component of the magnetic moment.

that of an orbital order domain in the CE-type phase, and consists of neighboring orthorhombic unit cells along the [110] direction, with two  $\text{Mn}^{4+}$  ions—hence bipolarons—situated between orbitally ordered  $\text{Mn}^{3+}$  ions. This CE-type bipolaron can also be viewed as a ferromagnetic zigzag, which is consistent with the observation of ferromagnetic fluctuations in  $\text{Pr}_{1-x}\text{Ca}_x\text{MnO}_3$  for the nearby doping range of  $x \approx 0.35-0.5$ ,<sup>27</sup> and with the absence of antiferromagnetic correlations in  $\text{La}_{0.7}\text{Ca}_{0.3}\text{MnO}_3$ .<sup>15</sup> We note that the presence of such ferromagnetic zigzags was recently proposed based on transport measurements of polycrystalline  $\text{La}_{5/8}\text{Ca}_{3/8}\text{MnO}_3$ .<sup>10</sup> Another perspective would be to view the correlations as small islands of an insulating phase—consistent with the phase separation picture of Moreo *et al.*<sup>28</sup>—although such a picture does not naturally explain either the size of the regions or the fact that it remains constant until the correlations disappear at high temperatures. We also note that our results are inconsistent with the theoretical, bipolaron model described earlier,<sup>9</sup> in that two holes on the same ion would result in a much shorter correlation length than the measured value of 1–2 lattice constants. In addition, a competing structure that has recently been proposed<sup>29,30</sup>—the orbital polaron, in which a  $\text{Mn}^{4+}$  ion is surrounded by six  $\text{Mn}^{3+}$  ions with their occupied  $e_g$  ( $3d_{z^2-r^2}$ ) orbitals pointing toward the central  $\text{Mn}^{4+}$  ion—is inconsistent with the wave vector reported here. To summarize, the proposed CE-type bipolaron structure is consistent with known experimental results, but it is not unique and alternative structures could also be constructed. In the future, experiments that explore the stability of these regions to other perturbations—such as doping or applied field—will be required to determine which, if any, of the pictures is the most appropriate.

The difference in the relative strength of the electron-phonon coupling for the two samples is manifested only at low temperatures, below the respective transition temperatures. As the  $\text{La}_{0.7}\text{Ca}_{0.3}\text{MnO}_3$  sample is cooled through the metal-insulator transition, the (1.5 2 0) intensity decreases with no change in the correlation length. This is consistent with the CE-type bipolaron picture described above, in which localization of correlated charge carriers is destroyed as the sample becomes conducting. It is also broadly consistent with a phase separation picture,<sup>28</sup> in which charge inhomogeneous and ferromagnetic metallic phases compete above the transition temperature. In contrast, in  $\text{Pr}_{0.7}\text{Ca}_{0.3}\text{MnO}_3$ , the (1.5 2 0) intensity grows and the width decreases as the sample goes through the charge and orbital order transition temperature. A plausible scenario for the transition in this case is that the number of CE-type bipolarons increases until they begin to coalesce, eventually forming orbitally ordered domains. This increase in the number of CE-type bipolarons could perhaps be driven by charge order fluctuations, consistent with the phenomenology re-

ported for the  $x=0.4$  and 0.5 dopings in this system.<sup>31,32</sup> The observation of low-temperature, resolution-limited, charge order peaks using the high-resolution Ge(111) analyzer at the (030) peak—in marked contrast to the short-range ordered orbital peaks—lends support to this scenario.

In conclusion, we have studied two CMR materials that differ only with respect to their trivalent cation species. A comparison of the high- and low-temperature behaviors underscores the importance of the electron-phonon coupling in such materials. In the high-temperature, paramagnetic, insulating phases, the behaviors of the polarons are found to be remarkably similar. That is, as the temperature is reduced toward the transition temperature, a slight increase in the number of correlated polarons is observed at the same (0.5 0 0)/(0 0.5 0)-type ordering wavevectors, and each with similar correlation lengths of 1–2 lattice constants in the two materials. This correlation length remains constant as long as the correlations persist—up to  $\sim 400$  K in  $\text{La}_{0.7}\text{Ca}_{0.3}\text{MnO}_3$ . The correlated polarons are consistent with a CE-type structure, and the similar behaviors in the two samples suggest that these correlated polarons are robust with respect to variations in the relative strength of the electron-phonon coupling.

The similarity in the behavior of the two samples breaks down upon cooling through their respective transition temperatures, as the small difference in the size of the trivalent cations—reflected in the relative strength of the electron-phonon coupling—becomes important. Below their transition temperatures,  $\text{La}_{0.7}\text{Ca}_{0.3}\text{MnO}_3$  becomes a ferromagnetic metal and  $\text{Pr}_{0.7}\text{Ca}_{0.3}\text{MnO}_3$  becomes a charge and orbitally ordered insulator. In  $\text{La}_{0.7}\text{Ca}_{0.3}\text{MnO}_3$ , the collapse of the correlated polarons can be attributed to the onset of ferromagnetic ordering, at which the energy gain associated with the ferromagnetic state overcomes the localization of the pairs of charge carriers caused by the electron-phonon coupling. In  $\text{Pr}_{0.7}\text{Ca}_{0.3}\text{MnO}_3$ , which has the stronger electron-phonon coupling, cooling through the transition temperature results instead in an ordering of the correlated polarons. The driving mechanism for this ordering is as yet unknown, but charge ordering is a candidate and will be the subject of future experiments.

The work at Brookhaven, both in the Physics Department and at the NSLS, was supported by the U.S. Department of Energy, Division of Materials Science, under Contract No. DE-AC02-98CH10886, and at Princeton University by the National Science Foundation under Grant No. DMR-9701191. Work at the CMC beamlines is supported, in part, by the Office of Basic Energy Sciences of the U.S. Department of Energy and by the National Science Foundation, Division of Materials Research. Use of the Advanced Photon Source was supported by the Office of Basic Energy Sciences of the U.S. Department of Energy under Contract No. W-31-109-Eng-38.

- <sup>1</sup>For a review, see *Colossal Magnetoresistive Oxides*, edited by Y. Tokura (Gordon & Breach, London, 1999).
- <sup>2</sup>C. Zener, *Phys. Rev.* **82**, 403 (1951); P. W. Anderson and H. Hasegawa, *ibid.* **100**, 675 (1955); P. G. deGennes, *ibid.* **118**, 141 (1960).
- <sup>3</sup>H. Röder, J. Zang, and A. R. Bishop, *Phys. Rev. Lett.* **76**, 1356 (1996).
- <sup>4</sup>A. J. Millis, B. I. Shraiman, and R. Mueller, *Phys. Rev. Lett.* **77**, 175 (1996).
- <sup>5</sup>M. F. Hundley, M. Hawley, R. H. Heffner, Z. X. Jia, J. J. Neumeier, J. Tesmer, J. D. Thompson, and X. D. Wu, *Appl. Phys. Lett.* **67**, 860 (1995).
- <sup>6</sup>M. Jaime, H. T. Hardner, M. B. Salamon, M. Rubinstein, P. Dorsey, and D. Emin, *Phys. Rev. Lett.* **78**, 951 (1997).
- <sup>7</sup>S. J. L. Billinge, R. G. DiFrancesco, G. H. Kwei, J. J. Neumeier, and J. D. Thompson, *Phys. Rev. Lett.* **77**, 715 (1996).
- <sup>8</sup>A. Shengalaya, G. Zhao, H. Keller, and K. A. Müller, *Phys. Rev. Lett.* **77**, 5296 (1996).
- <sup>9</sup>A. S. Alexandrov and A. M. Bratkovsky, *Phys. Rev. Lett.* **82**, 141 (1999).
- <sup>10</sup>K. H. Kim, M. Uehara, and S-W. Cheong, *Phys. Rev. B* **62**, R11 945 (2000).
- <sup>11</sup>G. M. Zhao, Y. S. Wang, D. J. Kang, W. Prellier, M. Rajeswari, H. Keller, T. Venkatesan, C. W. Chu, and R. L. Greene, *Phys. Rev. B* **62**, R11 949 (2000).
- <sup>12</sup>S. Shimomura, N. Wakabayashi, H. Kuwahara, and Y. Tokura, *Phys. Rev. Lett.* **83**, 4389 (1999).
- <sup>13</sup>L. Vasiliiu-Doloc, S. Rosenkranz, R. Osborn, S. K. Sinha, J. W. Lynn, J. Mesot, O. H. Seeck, G. Preosti, A. J. Fedro, and J. F. Mitchell, *Phys. Rev. Lett.* **83**, 4393 (1999).
- <sup>14</sup>P. Dai, J. A. Fernandez-Baca, N. Wakabayashi, E. W. Plummer, Y. Tomioka, and Y. Tokura, *Phys. Rev. Lett.* **85**, 2553 (2000).
- <sup>15</sup>C. P. Adams, J. W. Lynn, Y. M. Mukovskii, A. A. Arsenov, and D. A. Shulyatev, *Phys. Rev. Lett.* **85**, 3954 (2000).
- <sup>16</sup>J. M. Zuo and J. Tao, *Phys. Rev. B* **63**, 060407(R) (2001).
- <sup>17</sup>P. Schiffer, A. P. Ramirez, W. Bao, and S-W. Cheong, *Phys. Rev. Lett.* **75**, 3336 (1995).
- <sup>18</sup>Z. Jirak, S. Krupicka, Z. Simsa, M. Dlouha, and S. Vratilav, *J. Magn. Magn. Mater.* **53**, 153 (1985).
- <sup>19</sup>Y. Tomioka, A. Asamitsu, H. Kuwahara, Y. Moritomo, and Y. Tokura, *Phys. Rev. B* **53**, R1689 (1996).
- <sup>20</sup>The Mn-O-Mn bond angles are the in-plane, room temperature values. Data for  $\text{La}_{0.7}\text{Ca}_{0.3}\text{MnO}_3$  were interpolated from  $x=0.25$  and  $x=0.33$  results reported in Q. Huang, A. Santoro, J. W. Lynn, R. W. Erwin, J. A. Borchers, J. L. Peng, K. Ghosh, and R. L. Greene, *Phys. Rev. B* **58**, 2684 (1998). Data for  $\text{Pr}_{0.7}\text{Ca}_{0.3}\text{MnO}_3$  were reported in H. Y. Hwang, S-W. Cheong, P. G. Radaelli, M. Marezio, and B. Batlogg, *Phys. Rev. Lett.* **75**, 914 (1995).
- <sup>21</sup>A. J. Millis, P. B. Littlewood, and B. I. Shraiman, *Phys. Rev. Lett.* **74**, 5144 (1995).
- <sup>22</sup>T. Egami, in *Structure and Bonding*, Vol. 98, edited by J. B. Goodenough (Springer-Verlag, Berlin, 2001).
- <sup>23</sup>C. Martin, A. Maignan, M. Hervieu, and B. Raveau, *Phys. Rev. B* **60**, 12 191 (1999).
- <sup>24</sup>P. G. Radaelli, R. M. Ibberson, D. N. Argyriou, H. Casalta, K. H. Andersen, S-W. Cheong, and J. F. Mitchell, *Phys. Rev. B* **63**, 172419 (2001).
- <sup>25</sup>C. S. Nelson, M. v. Zimmermann, J. P. Hill, D. Gibbs, D. Casa, B. Keimer, Y. Tomioka, and Y. Tokura (unpublished).
- <sup>26</sup>The Lorentzian-squared lineshape was chosen for the quality of the fit, and no theoretical justification is provided.
- <sup>27</sup>R. Kajimoto, T. Kakeshita, Y. Oohara, H. Yoshizawa, Y. Tomioka, and Y. Tokura, *Phys. Rev. B* **58**, R11 837 (1998).
- <sup>28</sup>See, for example, A. Moreo, S. Yunoki, and E. Dagotto, *Science* **283**, 2034 (1999).
- <sup>29</sup>R. Kilian and G. Khaliullin, *Phys. Rev. B* **60**, 13 458 (1999).
- <sup>30</sup>T. Mizokawa, D. I. Khomskii, and G. A. Sawatzky, *Phys. Rev. B* **63**, 024403 (2001).
- <sup>31</sup>M. v. Zimmermann, J. P. Hill, D. Gibbs, M. Blume, D. Casa, B. Keimer, Y. Murakami, Y. Tomioka, and Y. Tokura, *Phys. Rev. Lett.* **83**, 4872 (1999).
- <sup>32</sup>M. v. Zimmermann, C. S. Nelson, J. P. Hill, D. Gibbs, M. Blume, D. Casa, B. Keimer, Y. Murakami, C.-C. Kao, C. Venkataraman, T. Gog, Y. Tomioka, and Y. Tokura, cond-mat/0007231, *Phys. Rev. B* (to be published).